

# Preparation and Photochemistry of Single Wall Carbon Nanotubes Having Covalently Anchored Viologen Units

Mercedes Alvaro, Carmela Aprile, Pedro Atienzar, and Hermenegildo Garcia\*

Instituto de Tecnología Química CSIC-UPV and Departamento de Química UPV,  
Avda de los Naranjos s/n, 46022 Valencia, Spain

Received: December 16, 2004; In Final Form: February 15, 2005

An asymmetrically substituted viologen (V) has been covalently anchored to single wall carbon nanotube (SWNT) through an ester linkage by reacting chlorinated purified SWNT with *N*-methyl-*N'*-(6-hydroxyhexyl)-4,4'-bipyridine. Spectroscopic evidence for the covalent bond of viologen in V-SWNT comes from the chemical shift of the  $-CH_2-O-CO-$  methylene group in  $^1H$  NMR and from the variations of the 1590 and 1380  $cm^{-1}$  bands in the Raman spectrum of the V-SWNT with respect to SWNT. The fact that the estimated quenching constant of the SWNT emission by viologen is about 2 orders of magnitude higher than the diffusion coefficient indicates the occurrence of a static quenching arising from the formation of a nonemissive viologen-SWNT complex. Laser flash photolysis shows the formation of viologen radical cation upon direct excitation of V-SWNT. The viologen moiety of V-SWNT is able to form a charge-transfer complex with 2,6-dimethoxynaphthalene (DMN) as evidenced by optical spectroscopy and, upon selective photoexcitation in the charge-transfer band, this V-DMN complex anchored to SWNT gives rise to the corresponding charge separated state decaying in the submillisecond time scales.

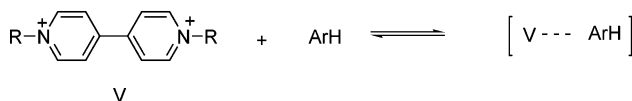
## Introduction

Given the promises of single wall carbon nanotubes (SWNT) in nanotechnology to develop responsive materials,<sup>1–4</sup> there is a current line of research aimed at the modification and control of the SWNT properties by introducing organic functionalities covalently attached to the SWNT.<sup>5</sup> Depending on the derivatization procedure, the appended groups can be preferentially located at the tips or at the graphene walls of the nanotube.<sup>5–7</sup> By means of this functionalization, the response of the nanotube upon external stimulus is expected to be controlled.

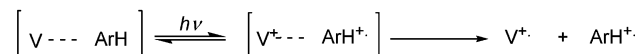
A type of probe molecules whose behavior has been studied in most of the supramolecular assemblies are viologens.<sup>8–10</sup> These heterocyclic cations are strong single electron acceptors that form easily detectable, long-lived radical cations.<sup>11–13</sup> Also viologens form charge-transfer (CT) complexes with many electron-rich molecules such as polycyclic aromatic hydrocarbons.<sup>11,12,14,15</sup> Formation of these CT complexes can be visually ascertained by the appearance of a yellow to orange color characteristic of these complexes. It is known that upon selective excitation, CT complexes undergo fast electron transfer from the electron-rich to the electron-poor component giving rise to geminal radical ion pairs.<sup>8,11,15–18</sup> These radical ion pairs may decay by back electron transfer between the geminal partners, or upon diffusing and escaping out-of-the-cage, the decay can take place by random radical ion recombination (Scheme 1). The main difference between the geminate and out-of-the-cage decay pathways is the time scale in which the two processes occur. Geminal ion pair recombination takes place in the subnanosecond time scale and is considered a waste of energy since the recombination is too rapid for other processes to compete. In contrast, escape out-of-the-cage generates a charge-separated state that can live in the millisecond time regime, allowing the possibility for other competitive chemical processes to occur within this lifetime.

## SCHEME 1: Photochemistry of CT Complexes between Viologen and Aromatic Compounds

(a) CT complex formation



(b) Photoinduced charge separation

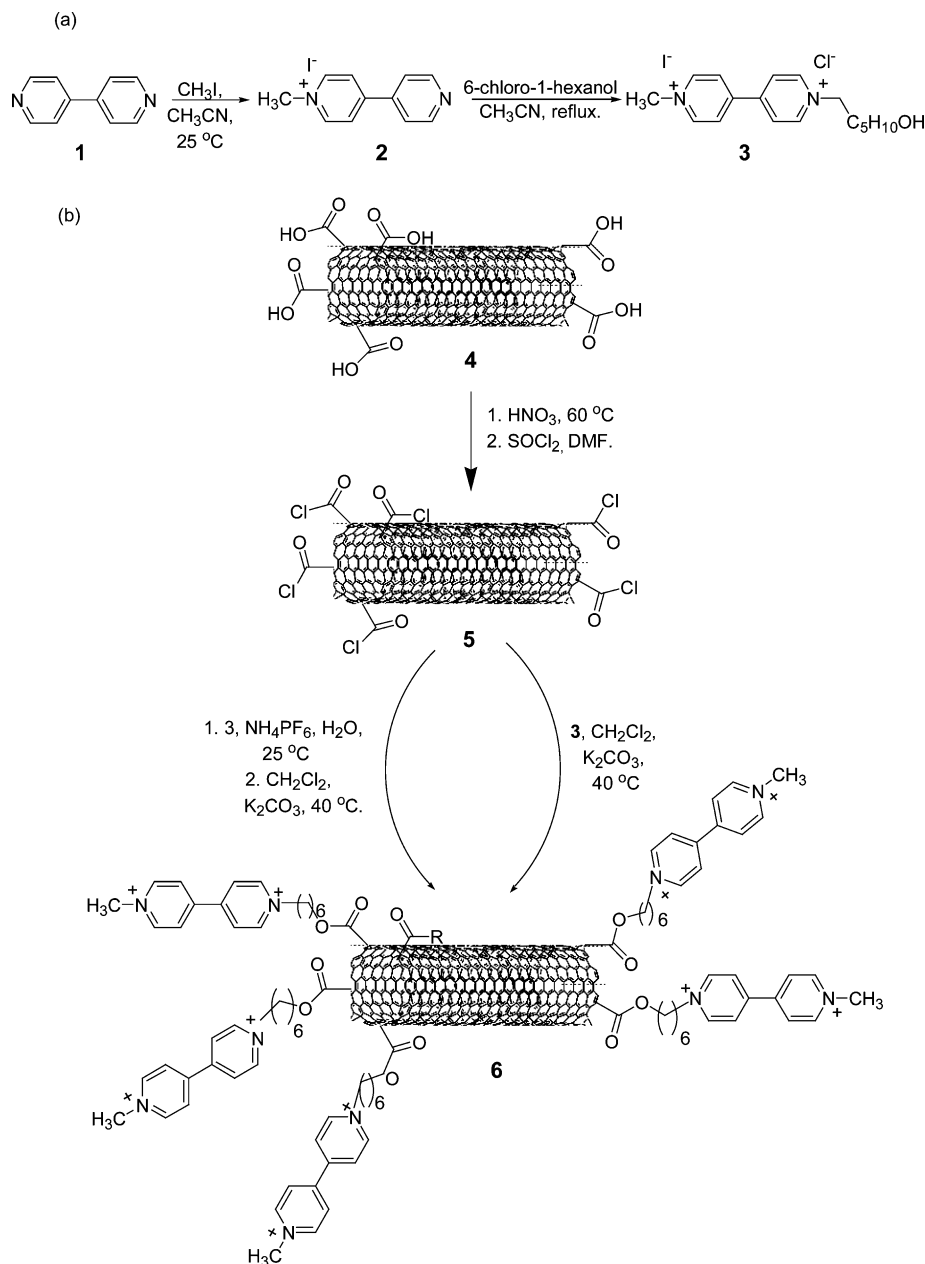


Given the importance of viologen in the formation of CT complexes as well as thermo-,<sup>19,20</sup> electro-,<sup>21–23</sup> and photochromic devices<sup>24,25</sup> and in photocatalysis<sup>26–31</sup> and solar light storage systems<sup>32,33</sup> we were interested in studying the properties of viologen covalently attached to SWNT, with the objective of finding some evidence for a photoinduced electron transfer between SWNT and the attached viologens.

## Results and Discussion

**(i) Preparation of V-SWNT.** Starting from a commercial SWNT that was purified from the metal catalyst by treatment with a 3 M  $HNO_3$  solution at 60 °C, the synthesis of V-SWNT was accomplished as indicated in Scheme 2. The key step in the synthesis is the preparation of an asymmetrically substituted *N,N'*-dialkylbipyridinium having a terminal OH group in one of the alkyl chains. This asymmetrically substituted viologen was prepared from 4,4'-bipyridine by an initial mono-*N*-methylation to give *N*-methylpyridinium **2**. This synthetic intermediate was submitted to a second alkylation with 6-chloro-1-hexanol (Scheme 2). The success of the stepwise *N*-alkylation arises from the very different nucleophilicity of bipyridine **1** and pyridinium

\* Address correspondence to this author. E-mail: hgarcia@qim.upv.es.

**SCHEME 2: (a) Synthesis of Asymmetrically Substituted Viologen 3 and (b) Purification and Chlorination of SWNT and Covalent Attachment of 3 to SWNT**

**2** due to the electron-withdrawing influence of the pyridinium moiety of **2** on the nitrogen electron lone pair of the pyridine unit. Thus, the first *N*-alkylation is considerably faster than the second one that requires more drastic conditions and longer reaction time to occur.

A notable property of viologen **3** having  $\text{I}^-$  as a counterion is its orange color, both in the solid state and in  $\text{CH}_2\text{Cl}_2$  solution. This color clearly indicates the presence of a CT complex between the bipyridinium cation as acceptor and iodide as electron donor. These types of halide–viologen complexes are well documented in literature, particularly when iodide is the accompanying halide due to its lower ionization potential.<sup>34–36</sup> To avoid the formation of this CT complex we proceeded to ion exchange iodide with  $\text{PF}_6^-$  using a saturated aqueous solution of ammonium hexafluorophosphate. The presence of  $\text{I}^-$  and the formation of the CT complex between V and  $\text{I}^-$  may play an undesirable influence on the interaction of V with the walls of the SWNT, thus modifying the efficiency of photochemical events. The success of the iodide exchange can be

visually assessed by the disappearance of the orange color, the resulting  $\text{PF}_6^-$  salt of the viologen precursor **3** being colorless.

Viologens having as counterion both  $\text{I}^-$  and  $\text{PF}_6^-$  were finally covalently attached through the terminal OH groups to the chlorinated SWNT. Additional details about the preparation of the viologen-modified nanotube V–SWNT as well as a pictorial illustration of its expected molecular structure can be found in Scheme 2 and in the Experimental Section.

It has been demonstrated that  $\text{SOCl}_2$  treatment of SWNT produces mainly the conversion of carboxylic groups generated during the oxidative purification step of SWNT to the corresponding acyl chlorides.<sup>37–40</sup> These carboxylic acid functionalities are mainly located at the tips of SWNT and therefore the covalent functionalization of these groups introduces the organic components predominantly at the opening of the tubes.

The resulting samples of V–SWNT were submitted to purification by dialysis to avoid the presence of residual organic precursors or other reagents not covalently bonded to the carbon nanotube.

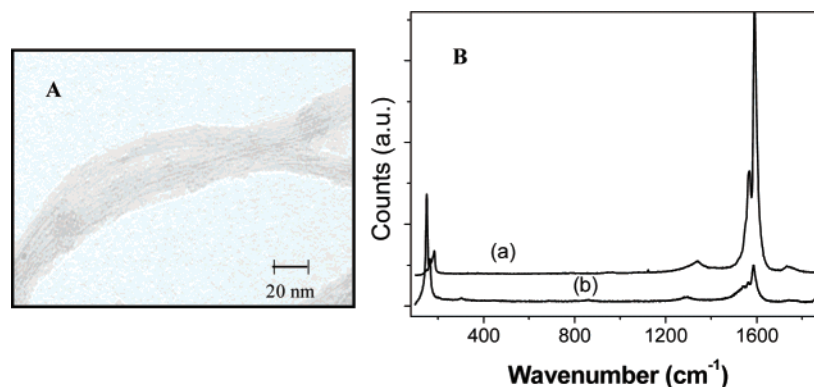


**Figure 1.** (A) TEM image of V-SWNT; (B) comparison of the FT-Raman spectra of initial SWNT (a) and that of V-SWNT (b).

**(ii) Characterization of Functionalized V-SWNT.** Experimental evidence of the successful formation of V-SWNT was obtained by combining the information derived from different spectroscopic, analytical, and microscopic techniques. Transmission electron microscopy (TEM) of V-SWNT shows that the typical single wall nanotube structure characteristic of pristine SWNT has been preserved through chemical treatment with somewhat reduced tendency of the nanotube to agglomerate forming bundles of tubes. This may be the consequence of the Coulombic repulsion between the V cations (Figure 1a). In addition to TEM, the nanotube structure of V-SWNT can also be deduced from the observation in Raman spectroscopy of the radial breathing mode appearing at  $320\text{ cm}^{-1}$  (Figure 1b). Comparing the Raman spectra of the original SWNT and that of the V-SWNT, we observed a blue shift in this radial breathing mode of  $30\text{ cm}^{-1}$  and, also important, a decrease in the intensity of the tangential vibration of the graphene wall at  $1590\text{ cm}^{-1}$  with the concomitant relative increase of a broad unresolved band at about  $1380\text{ cm}^{-1}$ .

These three features have been taken as hallmarks for covalent modification in SWNT and in case of massive functionalization even the complete disappearance of the narrow band at  $1590\text{ cm}^{-1}$  and concurrent growth in intensity of the broad band at  $1380\text{ cm}^{-1}$  has been recorded.<sup>41–44</sup> In our case the variations in the Raman spectra of V-SWNT compared with the unmodified nanotube are compatible with the preservation of nanotube structure with a moderate degree of functionalization.

For V-SWNT the nitrogen content is related exclusively to the presence of viologen. The N content was determined by combustion chemical analysis giving a value corresponding to 12 wt % of the viologen in the functionalized SWNT.

In agreement with the Raman information and with the viologen content determined by chemical analysis, the UV/vis spectrum of V-SWNT exhibits the presence of a peak at 280 nm that has been attributed to the presence of viologen by comparison with the optical spectrum of the original nanotube. Importantly the van Hoven singularities characteristic of the graphene walls are still observable in the near-IR region. The presence or the absence of van Hoven singularities depends on the degree of integrity of the graphene walls after the chemical functionalization and the fact that V-SWNT exhibits these absorption bands is again compatible with predominant functionalization at the tips rather than on the walls of the tubes.<sup>41,42</sup>

Given the percentage of viologen present in the V-SWNT sample, the macromolecular structure of SWNT, and the lower sensitivity of NMR spectroscopy as compared to the previous spectroscopic techniques, we anticipated a low signal-to-noise ratio in NMR spectra of the V-SWNT. Thus, the low sensitivity inherent to  $^{13}\text{C}$  NMR spectroscopy makes it impossible to record

the V-SWNT  $^{13}\text{C}$  NMR after prolonged acquisition time. Even the peaks corresponding to the carbons of the nanotube walls were not observable by  $^{13}\text{C}$  NMR spectroscopy. This finding could be related to the very inefficient spin relaxation in SWNT. In contrast, we were able to record a  $^1\text{H}$  NMR spectrum for V-SWNT in  $\text{CDCl}_3$  solution. The  $^1\text{H}$  NMR signals recorded for V-SWNT are compatible with the successful covalent attachment of the viologen unit to the nanotube. Of particular structural relevance is the chemical shift of the methylene group connected to an hydroxyl group in the viologen precursor **3** that becomes linked to an ester functionality after the covalent anchoring in V-SWNT. This change from  $-\text{OH}$  to  $-\text{OCOR}$  group should shift the  $-\text{CH}_2-$  signal about 0.5 ppm toward lower field.<sup>45</sup> In agreement with this structural change from compound **3** to V-SWNT,  $^1\text{H}$  NMR of V-SWNT showed no signals at 3.4 ppm corresponding to the viologen precursor **3** while two new triplets of relative intensity of 60/40 appear at 3.7 and 3.9 ppm, the triplet coupling being characteristic of a  $\text{CH}_2$  connected to a neighbor methylene group. The rest of the  $^1\text{H}$  NMR signals, especially the presence of aromatics at low field and their relative intensity, are also in agreement with the proposed structure of V-SWNT. The presence of two triplets instead of one could be related to the coexistence of two different chemical environments next to the ester moiety or it could be due to the influence of the nature of the counterion, either  $\text{PF}_6^-$  or  $\text{Cl}^-$ , on the methylene chemical shift. Chloride is introduced in the system during the chlorination of SWNT carboxylic acid and subsequent reaction of the acyl chloride. In fact, when an acyl chloride reacts a stoichiometric amount of  $\text{HCl}$  is liberated. In the chemistry of organic ionic compounds it is known that the nature of the counterion may strongly influence the NMR chemical shifts.<sup>46</sup> In support of this rationalization, it is worth noting that ion exchange from  $\text{Cl}^-$  to  $\text{PF}_6^-$  in precursor **3** produces a shift in the  $^1\text{H}$  NMR signals of the methylene group connected to the OH from 3.43 to 3.53 ppm.

**(iii) Photochemical Studies on V-SWNT.** After preparation and characterization of the sample we proceeded to the laser flash photolysis study of the V-SWNT sample with or without formation of a charge-transfer complex with 2,6-dimethoxynaphthalene as electron donor. As expected in view of the presence of viologen, 266 nm laser excitation gives rise to the formation of viologen radical cation as a transient decaying in the microsecond time scale. This  $\text{V}^{\bullet+}$  radical cation was characterized by the transient absorption spectrum consisting of a more intense absorption band at 390 nm together with a much broader, structured and less-intense band centered at 600 nm (Figure 2).<sup>47,48</sup> However, a closer inspection of the transient spectrum reveals that besides the  $\text{V}^{\bullet+}$  radical cation there must

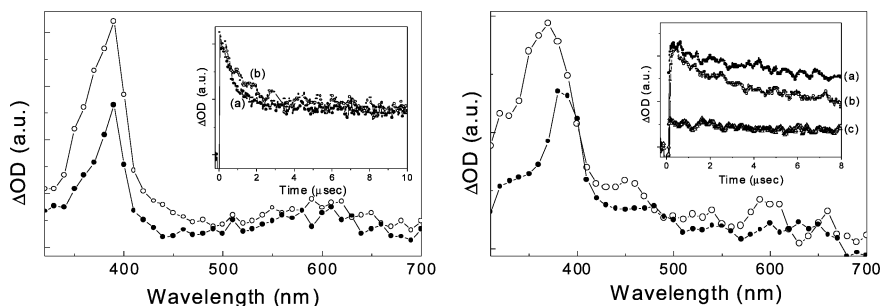


**Figure 2.** Left: Transient spectra recorded 0.6 and 7.5  $\mu\text{s}$  after 266 nm laser excitation of a  $\text{N}_2$  purged aqueous solution of compound **3** ( $10^{-2}$  M). The inset shows normalized signal decay monitored at 350 and 600 nm. Right: Transient spectra recorded 0.6 and 7.5  $\mu\text{s}$  after 266 nm laser excitation of a  $\text{N}_2$ -purged aqueous solution of V-SWNT (0.5 mg/mL). The inset shows the signal decay monitored at 360, 380, and 600 nm.

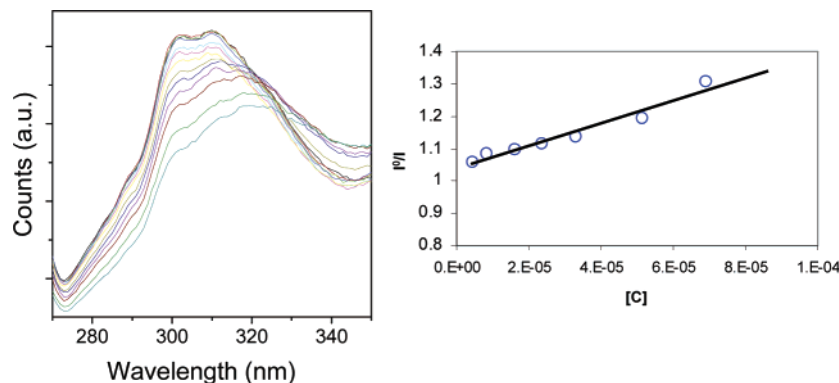


**Figure 3.** Left: Emission spectra of an aqueous V-SWNT solution ( $0.5 \text{ g L}^{-1}$ ) upon 266 nm excitation in the presence of increasing concentrations of viologen **3** as quencher. Right: Stern-Volmer plot of the relative emission intensity measured at 300 nm versus concentration of compound **3**.

be other transient species absorbing in the same time scale (compare in Figure 2 the left and right transient spectra).

The temporal profiles of the signals monitored at 380 and 600 nm for V-SWNT were not exactly coincident, indicating that the signals must correspond to more than a single species (see the inset of Figure 2 right). The estimated decay rate constants were  $3.7 \times 10^5$  and  $2.0 \times 10^5 \text{ s}^{-1}$  for the signal at 350 and 600 nm, respectively. As control, we also studied the photochemistry of the viologen precursor **3** under the same conditions. Comparison between the spectra and the temporal profiles of the V-SWNT and viologen precursor **3** shows remarkable differences in terms of spectra and temporal profiles. In the case of compound **3**, the signal temporal profiles monitored at 390 and 600 nm were coincident (being compatible with the formation of a single species) and decayed faster than those measured for V-SWNT ( $1 \times 10^6 \text{ s}^{-1}$ ). Particularly remarkable are the absorption in the 300–350 and 400–500 nm regions of transient arising from photoexcitation of V-SWNT that are absent in the spectrum of model compound **3**. These differences suggest that some SWNT transient species can be absorbing in these spectral regions. The presence of these transients supports the participation of SWNT in the photo-induced electron-transfer process leading to the generation of viologen radical cation when V-SWNT is photolyzed.

Interaction between V and SWNT is also supported in the SWNT quenching emission by the viologen precursor **3**. As reported in the literature,<sup>49,50</sup> SWNT can exhibit photoluminescence upon excitation in the UV region. It has been suggested that this luminescence arises from excitons localized at the walls defects having aromatic-like structure. As a matter of fact, excitation at 266 nm of SWNT allows the detection of an emission between 280 and 340 nm exhibiting the expected vibronic structure. This emission decays with a half-life of 3.6 ns obtained from the best fitting of the signal to a single monoexponential kinetics. This emission is quenched by addition

of increasing amounts of viologen precursor **3**; the estimated emission quenching constant  $k_q$  was obtained from the Stern-Volmer plot, giving a value of  $1.15 \times 10^{12} \text{ M}^{-1} \text{ s}^{-1}$ . This value is about 2 orders of magnitude higher than the diffusion coefficient of conventional molecules in acetonitrile.<sup>51</sup> It is expected that diffusion of macromolecular SWNT would be even much lower than low molecular weight solutes. Therefore, the high value estimated for  $k_q$  is indicating the occurrence of a static quenching rather than a dynamic quenching. The association constant roughly estimated from the quenching experiments is in the range of  $1000 \text{ M}^{-1}$ . Recent reports have shown that SWNT forms complexes with porphyrins, pyrene, and other compounds.<sup>52–56</sup> Our quenching study supports that this is also the case for viologens and it constitutes firm evidence of the interaction between the SWNT excited state and viologen **3**. Most probably, fluorescence quenching within the V-SWNT complex is a photoinduced electron transfer, this being compatible with the transient spectrum of V-SWNT upon 266 laser excitation shown in Figure 2 and leading to the formation of the  $\text{V}^{+\bullet}$  radical cation and some other SWNT transients.

As expected in view of previous work on related viologens, excitation of V-SWNT at 355 nm did not lead to the observation of any transient spectrum due to the fact that viologen has an absorption band at  $\lambda_{\text{max}}$  280 nm, the absorption at 355 nm being negligible. We use this negative result as a blank to compare the laser flash photolysis experiment of a CT complex between the 2,6-dimethoxynaphthalene (DMN) as donor and the viologen moiety of V-SWNT as acceptor. Formation of the CT complex was determined, as usual,<sup>11,15</sup> by monitoring in the optical spectrum the appearance of a structureless broad band from 350 to 450 nm specific of the CT complex whose intensity increases upon addition of increasing concentrations of DMN to V-SWNT.

In agreement with all the previous reports about the interaction of electron-rich arenes and viologen,<sup>11,15</sup> the characteristic



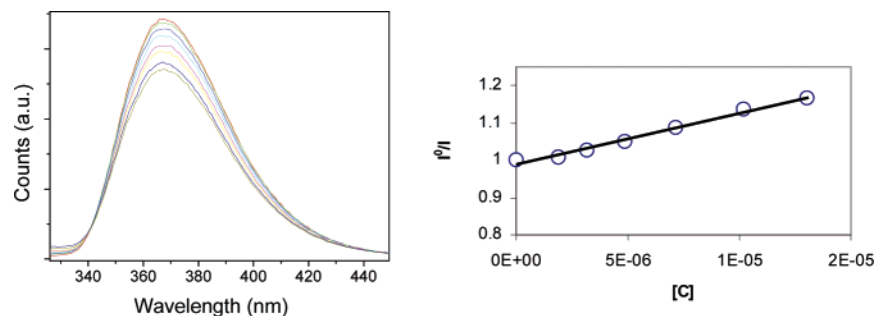


**Figure 4.** Left: Fluorescence spectra ( $\lambda$  excitation 320 nm) for an acetonitrile solution of DMN ( $10^{-4}$  M) upon addition of increasing amounts of V-SWNT. Right: Stern-Volmer plot of the relative emission intensity measured at 370 nm vs the concentration of V-SWNT.

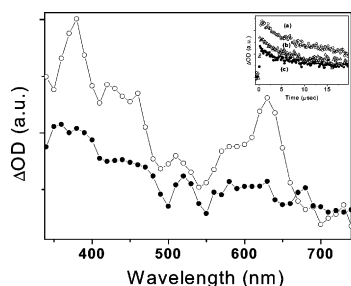


**Figure 5.** Transient spectra recorded 2.5 and 20  $\mu$ s after 266 nm laser excitation of N<sub>2</sub> purged with aqueous solution of compound 3 ( $10^{-2}$  M). The inset shows normalized signal decay monitored at 350 (a), 600 (b), and 630 nm (c).

emission of DMN is quenched by addition of increasing amounts of V-SWNT, the quenching rate constant being  $1.37 \times 10^{12} \text{ M}^{-1} \text{ s}^{-1}$  determined from the decrease in fluorescence intensity of the emission. Figure 4 shows the emission spectra from which  $k_q$  has been determined. As commented before, this  $k_q$  value higher than the diffusion coefficient indicates the formation of a complex between the fluophore and the quencher.

Upon laser flash excitation at the CT complex band of the DMN/V-SWNT complex using 355 nm it was possible to observe a transient spectra decaying in the microsecond time scale. This transient spectrum is compatible with the simultaneous generation of  $\text{DMN}^{\bullet+}$  ( $\lambda_{\text{max}} = 630$ )<sup>11</sup> and  $\text{V}^{\bullet+}$  ( $\lambda_{\text{max}} = 390$  and 600 nm). Figure 5 shows the transient spectra recorded for V-SWNT and the temporal profile corresponding to the disappearance of  $\text{DMN}^{\bullet+}$  and  $\text{V}^{\bullet+}$ . In agreement with earlier time-resolved measurements,<sup>57</sup> the decays in submillisecond time scale of the DMN radical cation and the V-SWNT radical cation do not coincide indicating that they correspond, at least in part, to non-geminate back electron transfer. The estimated decay rate constants were  $1.6 \times 10^5 \text{ s}^{-1}$  for the signal of  $\text{DMN}^{\bullet+}$  and  $1.3 \times 10^5 \text{ s}^{-1}$  for  $\text{V}^{\bullet+}$ .

## Conclusions

In the present work we have described the successful preparation of a single wall nanotube having covalently attached an asymmetric alkyl substituted viologen. Viologen forms a strong complex with the walls of the SWNT, leading to a static quenching of the SWNT emission. Laser flash photolysis leads to the corresponding viologen radical cation together with some extra absorption attributable to transient species arising from the SWNT. Viologen-modified SWNT forms a CT complex with electron donor compounds such as 2,6-dimethoxynaphthalene which exhibit the expected features of these CT complexes, i.e., absorption in the visible region and photo-induced electron transfer between the two partners.

## Experimental Section

All the solids were analyzed by combustion chemical analysis performed in a FISON CHNOS analyzer. FT-IR spectra were recorded with a Nicolet 710 FT-IR spectrophotometer. The IR spectra were recorded at room temperature under vacuum after outgassing the sample at 200 °C.

Laser flash photolysis experiments were carried out with the fourth (266 nm) or third (355 nm) harmonic of a Q-switched Nd:YAG laser (Spectron Laser Systems, UK; pulse width ca. 9 ns and 20 mJ pulse<sup>-1</sup>). The signal from the monochromator/photomultiplier detection system was captured by a Tektronix TDS640A digitizer and transferred to a PC computer that controlled the experiment and provided suitable processing and data storage capabilities. The TEM experiments were carried out with a Philips CM300 FEG system with an operating voltage of 100 kV. The Raman measurements (Renishaw inVia Raman Microscope) were carried out at room temperature with the 514.5 nm line of an Ar ion laser as an excitation source.

Diffuse reflectance UV/vis spectroscopy was performed using a Cary 5G adapted with a praying mantis accessory and with BaSO<sub>4</sub> as standard. <sup>1</sup>H and <sup>13</sup>C NMR were recorded in CDCl<sub>3</sub> as solvent with TMS as internal standard in a Varian Gemini 3000 (300 MHz).

**Purification and Chlorination of the Commercial HiPCO Single Wall Nanotube (SWNT).** The nanotube (100 mg) was suspended in a 3 M solution of nitric acid (5 mL) and stirred at 80 °C for 14 h. Then the suspension was filtered under vacuum with a Teflon membrane of 0.2  $\mu$ m and the solid exhaustively washed first with deionized water then with ether and finally dried under reduced pressure. The purified nanotube was obtained with a loss in weight of 40%.

Formation of the chlorinated SWNT was accomplished by suspending purified nanotube (100 mg) in SOCl<sub>2</sub> (10 mL). The mixture was stirred at 65 °C for 24 h and then cooled at room temperature. The solid was allowed to settle down and the SOCl<sub>2</sub> was cautiously removed. THF was added and the mixture was filtered under vacuum and washed with additional THF.

**Synthesis of 1-Methyl-4-(4'-pyridyl)pyridinium (2).** 4,4'-Bipyridine (800 mg, 5.12 mmol) was dissolved in dry acetonitrile (10 mL) and a solution of methyl iodide (0.320 mL, 5.12 mmol) in dry acetonitrile (10 mL) was slowly added. The mixture was stirred at room temperature for 8 h until complete disappearance of bipyridine and formation of the orange solid. Then the solvent was removed under reduced pressure to give an orange solid that is a mixture of monosubstituted and disubstituted bipyridine. The pure monosubstituted compound was obtained by treating the solid with acetonitrile, filtering the suspension, collecting the solution, and removing the solvent under reduced pressure. Compound 2 was obtained with a yield of 60%. <sup>1</sup>H NMR (CD<sub>3</sub>OD)  $\delta$  4.27 (s, 3H, CH<sub>3</sub>), 7.79 (dd,  $J$  =

1.5 and 4.5 Hz, 2H, ArH), 8.27 (d,  $J = 6.9$  Hz, 2H, ArH), 8.65 (d,  $J = 6.0$  Hz, 2H, ArH), 8.80 (d,  $J = 6.9$  Hz, 2H, ArH).  $^{13}\text{C}$  NMR ( $\text{CD}_3\text{OD}$ )  $\delta$  61.2, 122.2, 125.6, 126.4, 142.4, 145.2, 149.7.

**Synthesis of 1-(6-Hydroxyhexyl)-1'-methyl-(4,4')-bipyridinium (3).** Compound **2** (200 mg, 0.69 mmol) was dissolved in methanol (5 mL) and 6-chloro-1-hexanol (0.140 mL, 1.05 mmol) was added at room temperature. The mixture was stirred at reflux temperature for 48 h, then cooled at room temperature. The orange solid was purified by simple filtration and exhaustive washing with acetonitrile to remove the residual alcohol and 1-methyl-4-(4'-pyridyl)pyridium.  $^1\text{H}$  NMR ( $\text{D}_2\text{O}$ )  $\delta$  1.20–1.27 (m, 4H), 1.28–1.35 (m, 2H), 1.96–2.20 (m, 2H) 3.43 (t,  $J = 6.8$  Hz, 2H,  $\text{CH}_2\text{OH}$ ), 4.39 (s, 3H,  $\text{CH}_3$ ), 4.68 (t, 2H,  $\text{NCH}_2$ , overlapped with  $\text{D}_2\text{O}$  signal), 8.28 (t,  $J = 6.6$  and 6.3 Hz, 4H, ArH), 8.94 (d,  $J = 6.6$  Hz, 2H, ArH), 9.00 (d,  $J = 6.4$  Hz, 2H, ArH).  $^{13}\text{C}$  NMR ( $\text{D}_2\text{O}$ )  $\delta$  24.3, 24.8, 30.3, 30.7, 47.8, 48.2, 61.2, 122.7, 125.7, 126.5, 126.8, 142.6, 144.2, 145.5, 146.1, 148.9, 152.0.

**$\text{PF}_6^-$  Ion Exchange.** To exchange the iodide and chloride counterions present in as-synthesized compound **3** by  $\text{PF}_6^-$ , compound **3** was dissolved in water and a saturated solution of  $\text{NH}_4\text{PF}_6$  was added until complete precipitation of a white solid occurred. The ion exchange takes place in almost quantitative yield.  $^1\text{H}$  NMR ( $\text{CD}_3\text{CN}$ )  $\delta$  1.27–1.40 (m, 4H), 1.97–2.01 (m, 4H), 3.2 (s, OH), 3.53 (t,  $J = 6.8$  Hz, 2H,  $\text{CH}_2\text{OH}$ ), 4.44 (s, 3H,  $\text{CH}_3$ ), 4.68 (t,  $J = 7.2$  Hz, 2H,  $\text{NCH}_2$ ), 8.36 (d,  $J = 6.6$  Hz, overlapped with another d,  $J = 6.6$  Hz, 4H, ArH), 8.88–8.93 (m, 4H, ArH).  $^{13}\text{C}$  NMR ( $\text{CD}_3\text{CN}$ )  $\delta$  24.2, 24.8, 27.0, 35.7, 40.7, 48.5, 63.8, 126.2, 128.4, 129.7, 142.4, 145.5, 148.9.

**Functionalization of SWNT.** Compound **3** (50 mg) was dissolved in dichloromethane (10 mL), then the chlorinated SWNT (200 mg) and  $\text{K}_2\text{CO}_3$  were sequentially added. The mixture was stirred for 20 h at reflux temperature then cooled at room temperature and filtered. The solid was washed with methanol and dichloromethane. V-SWNT was dialyzed for 3 days with use of a membrane and water as solvent. After drying we obtained the V-SWNT with a loading of 12% calculated from combustion chemical analysis.  $^1\text{H}$  NMR ( $\text{CD}_3\text{CN}$ )  $\delta$  most characteristic signals: 3.72–3.78 (m, 3H), 3.84–3.90 (m, 2H), 4.58 (s,  $\text{CH}_3$ ), 8.28 (d, 2H, ArH), 8.20 (d, 2H, ArH), 8.25 (d, 2H, ArH), 8.68–8.73 (m, 4H, ArH). Even 1 day accumulation time did not lead to signals in  $^{13}\text{C}$  NMR spectroscopy.

**Acknowledgment.** Financial support by the Spanish Ministry of Science and Technology (MAT 2003-1226) is gratefully acknowledged. Carmela Aprile thanks the Ana y José Royo foundation for a postdoctoral scholarship. Pedro Atienzar thanks the Spanish Ministry of Science and Technology for a postgraduate scholarship. We also thank Manuel Planes for his technical assistance in acquiring the TEM images.

## References and Notes

- (1) Kuzmany, H.; Kukovec, A.; Simon, F.; Holzweber, M.; Kramberger, C.; Pichler, T. *Synth. Met.* **2004**, *141*, 113.
- (2) Colbert, D. T. *Plast. Addit. Compd.* **2003**, *5*, 18.
- (3) Nikolaev, P. J. *Nanosci. Nanotechnol.* **2004**, *4*, 307.
- (4) Rao, C. N. R.; Govindaraj, A. *Acc. Chem. Res.* **2002**, *35*, 998.
- (5) Hirsch, A. *Angew. Chem., Int. Ed.* **2002**, *41*, 1853.
- (6) Chen, Z.; Nagase, S.; Hirsch, A.; Haddon, R. C.; Thiel, W.; Schleyer, P. v. R. *Angew. Chem., Int. Ed.* **2004**, *43*, 1552.
- (7) Maynor, B. W.; An, L.; Lu, C.; Li, J.; Liu, J. *Abstracts of Papers*; 226th National Meeting of the American Chemical Society, New York, Sept 7–11, 2003; American Chemical Society: Washington, DC, 2003; INOR.
- (8) Clennan, E. L. *Coord. Chem. Rev.* **2004**, *248*, 477.
- (9) Sliwa, W.; Bachowska, B.; Zelichowicz, N. *Heterocycles* **1991**, *32*, 2241.
- (10) Turro, N. J.; Barton, J. K.; Tomalia, D. *Photochem. Convers. Storage Sol. Energy [Proc. Int. Conf.] 8th* **1991**, 121.
- (11) Garcia, H.; Roth, H. D. *Chem. Rev.* **2002**, *102*, 3947.
- (12) Tsukahara, K. *Trends Inorg. Chem.* **1991**, *2*, 17.
- (13) Alvaro, M.; Garcia, H.; Garcia, S.; Marquez, F.; Scaiano, J. C. *J. Phys. Chem.* **1997**, *101*, 3043.
- (14) Yoon, K. B.; Kochi, J. K. *J. Am. Chem. Soc.* **1989**, *111*, 1128.
- (15) Yoon, K. B. *Chem. Rev.* **1993**, *93*, 321.
- (16) Sankararaman, S.; Yoon, K. B.; Yabe, T.; Kochi, J. K. *J. Am. Chem. Soc.* **1991**, *113*, 1419.
- (17) Yabe, T.; Kochi, J. K. *J. Am. Chem. Soc.* **1992**, *114*, 4491.
- (18) Yoon, K. B.; Hubig, S. M.; Kochi, J. K. *J. Phys. Chem.* **1994**, *98*, 3865.
- (19) Alvaro, M.; Ferrer, B.; Fornes, V.; Garcia, H. *ChemPhysChem* **2003**, *4*, 612.
- (20) Suzuki, M.; Kimura, M.; Shirai, H. *Chem. Commun.* **1997**, 2061.
- (21) Mortimer, R. J. *Electrochim. Acta* **1999**, *44*, 2971.
- (22) Mortimer, R. J. *Chem. Soc. Rev.* **1997**, *26*, 147.
- (23) Somani, P. R.; Radhakrishnan, S. *Mater. Chem. Phys.* **2003**, *77*, 117.
- (24) Chen, Y. L.; Guan, Y. J.; Mai, Y. L.; Li, W.; Liang, Z. X. *J. Macromol. Sci., Chem.* **1988**, *A25*, 201.
- (25) Kamogawa, H. *Appl. Photochromic Polym. Syst.* **1992**, 207.
- (26) Lee, H.; Dutta, P. K. *J. Phys. Chem. B* **2002**, *106*, 11898.
- (27) Vitale, M.; Castagnola, N. B.; Ortins, N. J.; Brooke, J. A.; Vaidyalgam, A.; Dutta, P. K. *J. Phys. Chem. B* **1999**, *103*, 2408.
- (28) Das, S. K.; Dutta, P. K. *Langmuir* **1998**, *14*, 5121.
- (29) Castagnola, N. B.; Dutta, P. K. *J. Phys. Chem. B* **1998**, *102*, 1696.
- (30) Dutta, P. K.; Incavo, J. A. *J. Phys. Chem.* **1987**, *91*, 4443.
- (31) Dutta, P. K.; Borja, M.; Ledney, M. *Sol. Energy Mater. Sol. Cells* **1995**, *38*, 239.
- (32) Borja, M.; Dutta, P. K. *Nature* **1993**, *362*, 43.
- (33) Castagnola, N. B.; Dutta, P. K. *J. Photogr. Sci.* **1999**, *6*, 91.
- (34) Alvaro, M.; Ferrer, B.; Garcia, H.; Hashimoto, S.; Hiratsuka, M.; Asahi, T.; Masuhara, H. *ChemPhysChem* **2004**, *5*, 1058.
- (35) Pace, A.; Clennan, E. L.; Jensen, F.; Singleton, J. *J. Phys. Chem. B* **2004**, *108*, 4673.
- (36) Monk, P. M. S.; Hodgkinson, N. M.; Partridge, R. D. *Dyes Pigm.* **1999**, *43*, 241.
- (37) Dettlaff-weglikowska, U.; Skakalova, V.; Graupner, R.; Ley, L.; Roth, S. *Mater. Res. Soc. Symp. Proc.* **2003**, *772*, 179.
- (38) Della Negra, F.; Meneghetti, M.; Menna, E. *Fullerene Nanotube Carbon Nanostruct.* **2003**, *11*, 25.
- (39) Georgakilas, V.; Kordatos, K.; Prato, M.; Guldi, D. M.; Holzinger, M.; Hirsch, A. *J. Am. Chem. Soc.* **2002**, *124*, 760.
- (40) Holzinger, M.; Vostrowsky, O.; Hirsch, A.; Hennrich, F.; Kappes, M.; Weiss, R.; Jellen, F. *Angew. Chem., Int. Ed.* **2001**, *40*, 4002.
- (41) Saito, R.; Kataura, H. *Top. Appl. Phys.* **2001**, *80*, 213.
- (42) Saito, R.; Grueneis, A.; Samsonidze, G. G.; Dresselhaus, G.; Dresselhaus, M. S.; Jorio, A.; Cancado, L. G.; Pimenta, M. A.; Souza Filho, A. G. *Appl. Phys. A* **2004**, *A78*, 1099.
- (43) Dresselhaus, M. S.; Dresselhaus, G.; Jorio, A.; Souza Filho, A. G.; Saito, R. *Carbon* **2002**, *40*, 2043.
- (44) Jorio, A.; Pimenta, M. A.; Souza Filho, A. G.; Saito, R.; Dresselhaus, G.; Dresselhaus, M. S. *New J. Phys.* **2003**, *5*, 1.
- (45) Pretsch, E.; Clerc, T.; Seibl, J.; Simon, W. *Tables of Spectral Data for Structure Determination of Organic Compounds:  $^{13}\text{C}$  NMR,  $^1\text{H}$  NMR, IR, MS, UV/VIS. Chemical Laboratory Practice*; Springer-Verlag: New York, 1983.
- (46) Lin, S.-T.; Ding, M.-F.; Chang, C.-W.; Lue, S.-S. *Tetrahedron* **2004**, *60*, 9441.
- (47) Alvaro, M.; Chretien, M. N.; Ferrer, B.; Fornes, V.; Garcia, H.; Scaiano, J. C. *Chem. Commun.* **2001**, 2106.
- (48) Alvaro, M.; Ferrer, B.; Fornes, V.; Garcia, H. *Chem. Commun.* **2001**, 2546.
- (49) Alvaro, M.; Atienzar, P.; Bourdelande, J. L.; Garcia, H. *Chem. Commun.* **2002**, 3004.
- (50) Alvaro, M.; Atienzar, P.; de la Cruz, P.; Delgado, J. L.; Garcia, H.; Langa, F. *Chem. Phys. Lett.* **2004**, *386*, 342.
- (51) Murov, S. L. *Handbook of Organic Photochemistry*; Marcel Dekker: New York, 1973.
- (52) Wu, W.; Liu, L.; Li, Y.; Guo, Z.-X.; Dai, L.; Zhu, D. *Fullerene Nanotube Carbon Nanostruct.* **2003**, *11*, 89.
- (53) Fernando, K. A. S.; Lin, Y.; Wang, W.; Kumar, S.; Zhou, B.; Xie, S.-Y.; Cureton, L. T.; Sun, Y.-P. *J. Am. Chem. Soc.* **2004**, *126*, 10234.
- (54) Guldi, D. M.; Rahman, G. M. A.; Jux, N.; Tagmatarchis, N.; Prato, M. *Angew. Chem., Int. Ed.* **2004**, *43*, 5526.
- (55) Guldi, D. M.; Rahman, G. N. A.; Ramey, J.; Marcaccio, M.; Paolucci, D.; Paolucci, F.; Qin, S.; Ford, W. T.; Balbinot, D.; Jux, N.; Tagmatarchis, N.; Prato, M. *Chem. Commun. (Cambridge, United Kingdom)* **2004**, 2034.
- (56) Murakami, H.; Nomura, T.; Nakashima, N. *Chem. Phys. Lett.* **2003**, *378*, 481.
- (57) Alvaro, M.; Corma, A.; Ferrer, B.; Garcia, H.; Palomares, E. *Phys. Chem. Chem. Phys.* **2004**, *6*, 1345.